

The molecular nature of superfluidity: Viscosity of helium from quantum stochastic molecular dynamics simulations over real trajectories

Phil Attard

phil.attard1@gmail.com July 2024–Feb. 2025

Using quantum equations of motion for interacting bosons, stochastic molecular dynamics simulations with quantized momenta are performed for Lennard-Jones helium-4. The viscosity of the quantum liquid is significantly less than that of the classical liquid, being almost 5 times smaller at the lowest temperature studied. The classical and quantum liquids are identical except for Bose-Einstein condensation, which pinpoints the molecular mechanism for superfluidity. The results rely on the existence of stochastic but real particle trajectories, which has implications for the interpretation of quantum mechanics.

I. INTRODUCTION

Shut up and calculate (1.1)

is an aphorism apparently due to Mermin, although some say Feynman (Mermin 1989, 2004). The sentiment, which is widespread and likely predates the specific phrase, suggests that it is a waste of time to speculate about the interpretation of quantum mechanics since everyone agrees upon the fundamental equations. It acknowledges the spookiness of quantum non-locality and the jittery state of Schrödinger's cat, but it insists that the physical meaning of these has no bearing on the application of the quantum laws and equations, which themselves are unambiguous.

It is certainly true that any theory or calculation is bound by the mathematical rules. Nevertheless I think that it goes too far to say that the physical interpretation of those rules is irrelevant or that the discussion of fundamental quantum concepts is mere sophistry. Once one goes beyond the highly idealized undergraduate textbook examples to work on real world problems, it is necessary to introduce approximations into the fundamental quantum equations. Such approximations may involve neglecting particular classes of terms while resumming others, defining parameters and taking small or large asymptotic limits, choosing specific functions for expansion series, imposing particular boundary conditions, etc. The approach chosen depends not just upon the physical characteristics of the problem at hand but also upon the interpretation of quantum mechanics that leads to an understanding of what is important and what is negligible, what is doable and what is forbidden. It is often the case that the real world application is so far removed from the fundamental quantum equations that the results of an early decision for the research direction cannot be fully anticipated or easily undone. Different interpretations can lead to widely divergent theories due to the sensitivity to the initial beliefs, if you will.

Let me give a concrete example that is directly relevant to the present paper on computing the viscosity of

helium in the superfluid regime. The Copenhagen interpretation of quantum mechanics holds that the world is not objectively real and that it only comes into existence when it is measured or observed. More specifically, particles only possess position or momentum at the time of measurement, and that only one of these can be measured at a time. Therefore, it is said, a particle does not possess simultaneously position and momentum. The corollary of this is that particles cannot follow a path from one position-momentum point to another, which is to say that particle trajectories do not exist.

Obviously any scientist who wishes to understand superfluidity at the molecular level and who believes in the Copenhagen interpretation of quantum mechanics would never consider developing a theory or approximation that is based upon real particles with actual positions and momenta following actual trajectories in time. This example illustrates how a particular interpretation of quantum mechanics can proscribe from the start the theories or approximations that are even considered, let alone explored.

The results in this paper are based on real particles with simultaneously specified positions and momenta, and on real molecular trajectories in time. These obviously contradict the Copenhagen interpretation of quantum mechanics. But do they contradict the equations of quantum mechanics? Obviously I argue not, as I now briefly explain.

It is certainly true that the position and momentum operators do not commute and that Heisenberg's uncertainty principle bounds the product of the variance of the expectation values of the position and momentum operators. These are indisputable mathematical facts. Anything beyond these is a matter of interpretation, and highly questionable interpretation at that. For example, the assertion that an expectation value is a measurement is dubious; there are entire journals devoted to the quantum theory of measurement and the only thing that the various authors agree upon is that a measurement is not simply an expectation value. Further, it is not at all clear that the lack of commutativity of the position and momentum operators implies the Copenhagen interpre-

tation that a particle cannot possess simultaneously a position and a momentum. For a counter-example, see the de Broglie-Bohm pilot wave theory, which reproduces all of the known results of quantum mechanics (Bohm 1952, de Broglie 1928, Goldstein 2024).

The approach used here is predicated on the interpretation that it is the momentum eigenvalue that gives the momentum of a particle, and that a momentum eigenfunction at a particular position should be interpreted as a complex number that is associated with the simultaneous specification of the position and momentum of the particle. In a way that will be made clear, the state of the system is the product of single-particle momentum eigenfunctions of the subsystem, and the subsystem evolves in time by following a trajectory through classical phase space as given by the Schrödinger equation applied to the momentum eigenfunctions and taking into account the interactions with the environment. It is essential to this approach that the subsystem of interest be open and that it can exchange energy and momentum with its environment. (The total system consists of the subsystem and the reservoir or environment.) It is also essential that the symmetrization of the wave function be explicitly accounted for.

At the end of the day, the present interpretation and the consequent approximations that are made should be judged by their physical plausibility and by the results that they produce. One cannot really maintain that the interpretation of quantum mechanics is irrelevant to the real world if the same starting equations combined with different interpretations lead to different quantitative descriptions of that world. The present approach gives a quantitative estimate of the shear viscosity of superfluid helium that includes molecular interactions. Apart from related work by the present author (Attard 2023b, 2025), these are the first such molecular-level results for the superfluid viscosity. It is therefore reasonable to conclude that the proximal impediment to the molecular understanding and quantitative description of superfluidity has been the Copenhagen interpretation of quantum mechanics.

II. ANALYSIS

A. Hamiltonian Dynamics

Quantum statistical mechanics may be formulated in classical phase space (Attard 2018, 2021, 2023a). This exact transformation relies upon decoherence due to entanglement with the reservoir or environment. This configuration picture invokes the momentum eigenfunction $\phi_{\mathbf{p}}(\mathbf{q}) = V^{-N/2} e^{-\mathbf{p} \cdot \mathbf{q}/i\hbar}$ (Merzbacher 1970, Messiah 1961). Here for N particles the momentum configuration is $\mathbf{p} = \{\mathbf{p}_1, \mathbf{p}_2, \dots, \mathbf{p}_N\}$, and the position configuration is $\mathbf{q} = \{\mathbf{q}_1, \mathbf{q}_2, \dots, \mathbf{q}_N\}$. The momenta are quantized, with momentum state spacing $\Delta_p = 2\pi\hbar/L$, with $V = L^3$ being the volume of the cubic subsystem, and

$\hbar = 1.05 \times 10^{-34} \text{Js}$ being Planck's constant divided by 2π . The spacing between momentum states goes to zero in the thermodynamic limit. Note that a point in classical phase space, $\Gamma \equiv \{\mathbf{q}, \mathbf{p}\}$, has the interpretation of a specific configuration of bosons at these positions with these (quantized) momenta, and it has associated with it the complex number $\phi_{\mathbf{p}}(\mathbf{q})$.

For bosons the normalized symmetrized momentum eigenfunction is

$$\phi_{\mathbf{p}}^+(\mathbf{q}) = \frac{1}{\sqrt{N! \chi_{\mathbf{p}}^+}} \sum_{\hat{\mathbf{P}}} \phi_{\hat{\mathbf{P}}\mathbf{p}}(\mathbf{q}), \quad (2.1)$$

$\hat{\mathbf{P}}$ being the permutation operator. The symmetrization factor is

$$\begin{aligned} \chi_{\mathbf{p}}^+ &= \sum_{\hat{\mathbf{P}}} \langle \phi_{\mathbf{p}} | \phi_{\hat{\mathbf{P}}\mathbf{p}} \rangle \\ &= \sum_{\hat{\mathbf{P}}} \delta_{\mathbf{p}, \hat{\mathbf{P}}\mathbf{p}} \\ &= \prod_{\mathbf{a}} N_{\mathbf{a}}(\mathbf{p})!. \end{aligned} \quad (2.2)$$

Here and throughout the occupancy of the single particle momentum state \mathbf{a} is $N_{\mathbf{a}} = \sum_{j=1}^N \delta_{\mathbf{p}_j, \mathbf{a}}$. This is what ultimately drives Bose-Einstein condensation (Attard 2025).

The Born probability associated with a point in classical phase space for the subsystem in a symmetrized decoherent momentum state is (Attard 2025 Eq. (5.67))

$$\begin{aligned} &\phi_{\mathbf{p}}^+(\mathbf{q})^* \phi_{\mathbf{p}}^+(\mathbf{q}) \\ &= \frac{1}{V^N N! \chi_{\mathbf{p}}^+} \sum_{\hat{\mathbf{P}}', \hat{\mathbf{P}}''} e^{-(\hat{\mathbf{P}}'\mathbf{p} - \hat{\mathbf{P}}''\mathbf{p}) \cdot \mathbf{q}/i\hbar} \\ &\approx \frac{1}{V^N N! \chi_{\mathbf{p}}^+} \sum_{\hat{\mathbf{P}}', \hat{\mathbf{P}}''} \sum_{\hat{\mathbf{P}}' \mathbf{p} \approx \hat{\mathbf{P}}'' \mathbf{p}} e^{-(\hat{\mathbf{P}}'\mathbf{p} - \hat{\mathbf{P}}''\mathbf{p}) \cdot \mathbf{q}/i\hbar}. \end{aligned} \quad (2.3)$$

The reason for neglecting the terms involving permutations of bosons with dissimilar momenta is that these are more or less randomly and uniformly distributed on the unit circle in the complex plane, and so they add up to zero. This is particularly the case when one considers that small changes in the positions may lead to wildly different exponents for any such permutations. The sum that is retained involves only permutations between bosons in the same, or nearly the same, momentum state, in which case the exponent is zero, or close to zero, even for small changes in positions. The number of permutations between bosons in exactly the same momentum states in the double sum is $\sum_{\hat{\mathbf{P}}', \hat{\mathbf{P}}''} (\hat{\mathbf{P}}'\mathbf{p} \approx \hat{\mathbf{P}}''\mathbf{p}) = N! \prod_{\mathbf{a}} N_{\mathbf{a}}(\mathbf{p})! = N! \chi_{\mathbf{p}}^+$. Arguably these are the ones that dominate, particularly on the low side of the λ -transition, which means that we may take $\phi_{\mathbf{p}}^+(\mathbf{q}) = \phi_{\mathbf{p}}(\mathbf{q})$.

An open system is decoherent (Attard 2018, 2021, Joos and Zeh 1985, Schlosshauer 2005, Zurek 1991). Decoherence means that the only allowed permutations must

satisfy $\hat{\mathbf{P}}\mathbf{p} = \mathbf{p}$. Otherwise the symmetrized momentum eigenfunction, $\phi_{\mathbf{p}}^+(\mathbf{q})$, would be a superposition of states.

There is a decoherence time τ_{mix} (Caldeira and Leggett 1983, Schlosshauer 2005, Zurek *et al.* 2003). This likely decreases with increasing distance between permuted momentum states.

Schrödinger's equation for the time evolution of the momentum eigenfunction in a decoherent system for a small time step gives (Attard 2023d, 2025),

$$[\hat{\mathbf{I}} + (\tau/i\hbar)\hat{\mathcal{H}}(\mathbf{q})]\phi_{\mathbf{p}}(\mathbf{q}) = \phi_{\mathbf{p}'}(\mathbf{q}'). \quad (2.4)$$

Time reversibility and continuity imply that

$$\begin{aligned} \mathbf{q}' &= \mathbf{q} + \tau \nabla_{\mathbf{p}} \mathcal{H}(\mathbf{q}, \mathbf{p}), \\ \text{and } \mathbf{p}' &= \mathbf{p} - \tau \nabla_{\mathbf{q}} \mathcal{H}(\mathbf{q}, \mathbf{p}). \end{aligned} \quad (2.5)$$

These are Hamilton's classical equations of motion. The second says that a boson's momentum evolves according to the classical force acting on it, $\dot{\mathbf{p}}_j = -\nabla_{\mathbf{q},j} \mathcal{H}(\mathbf{q}, \mathbf{p}) = \mathbf{f}_j$. Here it is implicitly assumed that the spacing between momentum states is small enough to allow the continuum approximation.

It should be emphasized that there are two sources of decoherence: there is the internal decoherence that was discussed above on the basis of the Born probability, and there is the external decoherence due to the entanglement of the open subsystem with the environment or reservoir. Both mechanisms dictate that the subsystem must be in a pure state where each boson has a position and a momentum. Allowed permutations are between bosons in the same momentum state. Those permutations which would correspond to the superposition of different momentum configurations are suppressed.

B. Newton's Second Law: The Condensed Version

For a momentum configuration \mathbf{p} in the condensed regime, the single-particle quantized momentum state \mathbf{a} is occupied by $N_{\mathbf{a}} = \sum_{j=1}^N \delta_{\mathbf{p}_j, \mathbf{a}}$ bosons. Let the n_A bosons in a specific subset $A \in \mathbf{a}$ be $A = \{j_1, j_2, \dots, j_{n_A}\}$, with $\mathbf{p}_{j_k} = \mathbf{a}$. The momentum eigenfunction for this subset is $\phi_{\mathbf{p}^{n_A}}(\mathbf{q}^{n_A})$. Let $\hat{\mathbf{P}}_A$ be one of the $n_A!$ permutations amongst the bosons in the specific subset A . Obviously the momentum configuration is unchanged by such a permutation, $\hat{\mathbf{P}}_A \mathbf{p}^{n_A} = \mathbf{p}^{n_A} = \mathbf{a}^{n_A}$. The Schrödinger time propagator for this subset yields

$$\begin{aligned} \left[\hat{\mathbf{I}} + \frac{\tau}{i\hbar} \hat{\mathcal{H}}(\mathbf{q}^{n_A}) \right] \phi_{\mathbf{p}^{n_A}}(\mathbf{q}^{n_A}) &= \phi_{\mathbf{p}'^{n_A}}(\mathbf{q}'^{n_A}) \\ &= \frac{1}{n_A!} \sum_{\hat{\mathbf{P}}_A} \phi_{\hat{\mathbf{P}}_A \mathbf{p}'^{n_A}}(\mathbf{q}'^{n_A}), \end{aligned} \quad (2.6)$$

since the left hand side is unchanged by the sum over permutations. This suggests that the subset moves rigidly, which is to say $\mathbf{p}'_{j_k} = \mathbf{a}'_A$ for $j_k \in A$, since this ensures that $\hat{\mathbf{P}}_A \mathbf{p}'^{n_A} = \mathbf{p}'^{n_A}$.

The *classical* equations of motion become

$$\begin{aligned} \mathbf{p}'^{n_A} &= \frac{1}{n_A!} \sum_{\hat{\mathbf{P}}_A} \hat{\mathbf{P}}_A \mathbf{p}'^{n_A} \\ &= \mathbf{p}^{n_A} + \frac{\tau}{n_A!} \sum_{\hat{\mathbf{P}}_A} \hat{\mathbf{P}}_A \mathbf{f}^{n_A} \\ &= \mathbf{p}^{n_A} + \tau \mathbf{F}_A^{n_A}. \end{aligned} \quad (2.7)$$

It is obvious that symmetrizing the force by permutation over the subset is equivalent to the average non-local force per boson for the subset, $\mathbf{F}_A \equiv (n_A!)^{-1} \sum_{\hat{\mathbf{P}}_A} \{ \hat{\mathbf{P}}_A \mathbf{f}^{n_A} \}_{j_k} = n_A^{-1} \sum_{j \in A} \mathbf{f}_j$.

There are ${}^{N_{\mathbf{a}}}C_{n_A} \equiv N_{\mathbf{a}}!/(N_{\mathbf{a}} - n_A)!n_A!$ ways of allocating labeled bosons from the momentum state \mathbf{a} with $N_{\mathbf{a}}$ bosons to a subset A with n_A bosons. Label these $n = 1, 2, \dots, {}^{N_{\mathbf{a}}}C_{n_A}$. Each one of these has an indistinguishable initial configuration, \mathbf{a}^{n_A} , but a different average non-local force \mathbf{F}_{A_n} and hence a different evolved configuration $\mathbf{p}_n^{n_A}$. The evolved configuration is a superposition of these. But as an open quantum system, it must collapse into a single configuration. The specific configuration occurs with probability $1/{}^{N_{\mathbf{a}}}C_{n_A}$, which means that the quantum equation of motion for the evolution of the specific subset of n_A bosons in the momentum state \mathbf{a} is

$$\mathbf{p}'^{n_A} = \mathbf{p}^{n_A} + \tau \frac{(N_{\mathbf{a}} - n_A)!n_A!}{N_{\mathbf{a}}!} \mathbf{F}_A^{n_A}, \quad (2.8)$$

where the A refers to a specific labeled subset of the ${}^{N_{\mathbf{a}}}C_{n_A}$ possible subsets.

We can confirm that this is correct and gain some insight into the physical process by looking at energy conservation. If the momentum state is divided into the subset A with n_A bosons, and A' with $n_{A'} = N_{\mathbf{a}} - n_A$ bosons, then the respective forces per boson are \mathbf{F}_A and $\mathbf{F}_{A'}$. The total force, $n_A \mathbf{F}_A + n_{A'} \mathbf{F}_{A'} = \sum_{j \in \mathbf{a}} \mathbf{f}_j$, is the same for each of the ${}^{N_{\mathbf{a}}}C_{n_A}$ possible A_n . The change in total potential energy over the time step for the bosons in \mathbf{a} is $\Delta U = -\tau \sum_{j \in \mathbf{a}} \mathbf{f}_j \cdot \mathbf{a}/m$ because there is just one position configuration. With the above condensed equation of motion the change in total kinetic energy for the superposed momentum states is

$$\begin{aligned} \Delta \mathcal{K} &= \frac{1}{m} \sum_{n=1}^{N_{\mathbf{a}}} \left\{ \mathbf{a}^{n_A} \cdot [\mathbf{p}_n'^{n_A} - \mathbf{a}^{n_A}] \right. \\ &\quad \left. + \mathbf{a}^{n_{A'}} \cdot [\mathbf{p}_n'^{n_{A'}} - \mathbf{a}^{n_{A'}}] \right\} \\ &= \frac{\tau}{m} \frac{n_A!n_{A'}!}{N_{\mathbf{a}}!} \sum_{n=1}^{N_{\mathbf{a}}} \left\{ n_A \mathbf{a} \cdot \mathbf{F}_{A_n} + n_{A'} \mathbf{a} \cdot \mathbf{F}_{A'_n} \right\} \\ &= \frac{\tau}{m} \sum_{j \in \mathbf{a}} \mathbf{a} \cdot \mathbf{f}_j. \end{aligned} \quad (2.9)$$

This cancels with the change in potential energy. Hence the superposed evolved momentum states maintain constant energy for the bosons originally in the momentum

state \mathbf{a} . It is essential for this result that the force on the subsets A and A' be reduced by the binomial coefficient.

The result for the evolution of the momentum of a subset of bosons, Eq. (2.8), says that Newton's classical rate of change of momentum is shared amongst the $N_{\mathbf{a}}C_{n_A}$ superposed states, which in total conserves energy. But since only one momentum configuration survives, we conclude that kinetic energy is lost to the environment via entanglement. This result explains physically the conditional transition probability derived next.

C. Adiabatic Stochastic Transition

The change in position of the bosons over a time step τ is deterministic,

$$\mathbf{q}(t + \tau) = \mathbf{q}(t) + \frac{\tau}{m}\mathbf{p}(t). \quad (2.10)$$

We now explicitly take the momenta to be quantized, with \mathbf{p} being a $3N$ -dimensional vector integer multiple of Δ_p .

As in the preceding §II B, we consider the transition of a subset A of bosons in the momentum state \mathbf{a} that moves rigidly according to the shared non-local force acting on the subset. The size distribution for the subsets will be derived in the following §II D.

The present rigid subset model allows the momentum state to break up and the bosons ties to rearrange according to the state that they occupy after each time step or even after each successful transition. This shifts from the occupancy picture to the configuration picture, and therefore changes in occupation entropy must be taken into account. The configuration probability density is (Attard 2025)

$$\varphi(\mathbf{\Gamma}) = \frac{1}{Z} e^{-\beta \mathcal{K}(\mathbf{p})} e^{-\beta U(\mathbf{q})} \prod_{\mathbf{a}} N_{\mathbf{a}}!, \quad (2.11)$$

where $\beta = 1/k_B T$ is the inverse temperature, $\mathcal{K}(\mathbf{p})$ is the kinetic energy, $U(\mathbf{q})$ is the potential energy, the commutation function has been neglected, and the occupancy of the momentum state \mathbf{a} is $N_{\mathbf{a}} = \sum_{j=1}^N \delta_{\mathbf{p}_j, \mathbf{a}}$. Also, a point in quantized phase space is $\mathbf{\Gamma} = \{\mathbf{q}, \mathbf{p}\}$, and the conjugate point with momenta reversed is $\mathbf{\Gamma}^\dagger = \{\mathbf{q}, -\mathbf{p}\}$.

Consider a specific subset $A \in \mathbf{a}$ of n_A bosons. The shared non-local force per boson in the subset is $\mathbf{F}_A = n_A^{-1} \sum_{j \in A} \mathbf{f}_j$. We seek the conditional transition probability of this subset to the neighboring momentum state in the direction of the α component of the force on the subset, namely from \mathbf{a} to $\mathbf{a}'_\alpha = \mathbf{a} + \text{sign}(\tau F_{A,\alpha}) \Delta_p \hat{\mathbf{x}}_\alpha$. Microscopic reversibility gives the ratio of conditional transition probabilities,

$$\begin{aligned} \frac{\varphi(\mathbf{\Gamma}'|\mathbf{\Gamma}; \tau)}{\varphi(\mathbf{\Gamma}^\dagger|\mathbf{\Gamma}'^\dagger; \tau)} &= \frac{\varphi(\mathbf{\Gamma}')}{\varphi(\mathbf{\Gamma})} \\ &= e^{(-n_A \beta / 2m)[a'^2 - a^2]} e^{(n_A \beta \tau / m) \mathbf{F}_A \cdot \mathbf{a}} \\ &\quad \times \frac{(N_{\mathbf{a}'} + n_A)!(N_{\mathbf{a}} - n_A)!}{N_{\mathbf{a}'}! N_{\mathbf{a}}!}. \end{aligned} \quad (2.12)$$

(This does not include the size probability distribution of the subsets; see §II D.) By inspection, this is satisfied by a conditional transition probability with the general form

$$\begin{aligned} \varphi(\mathbf{a}'_\alpha | \mathbf{a}, n_A, N_{\mathbf{a}}, N_{\mathbf{a}'_\alpha}) & \quad (2.13) \\ &= \lambda_{A,\alpha} g(n_A) \left(\frac{(N_{\mathbf{a}'_\alpha} + n_A)!}{N_{\mathbf{a}'_\alpha}!} \right)^{1-r} \left(\frac{(N_{\mathbf{a}} - n_A)!}{N_{\mathbf{a}}!} \right)^r \\ &\quad \times e^{(-n_A \beta / 2m)[a'^2_\alpha - a^2_\alpha] / 2} e^{(n_A \beta \tau / m) F_{A,\alpha} a_\alpha / 2} \\ &\Rightarrow \lambda_{A,\alpha} \frac{n_A! (N_{\mathbf{a}} - n_A)!}{N_{\mathbf{a}}!} \\ &\quad \times \left\{ 1 - \frac{n_A \beta \Delta_p}{2m} \text{sign}(\tau F_{A,\alpha}) a_\alpha + \frac{\beta \tau a_\alpha}{2m} \sum_{j \in A} f_{j,\alpha} \right\}. \end{aligned}$$

The exponential of the change in energy has been linearized here, although this is unnecessary and might in fact be ill-advised for larger subsets. In the particular solution that is the final equality, $r = 1$ has been chosen. Likewise, $g(n_A) = n_A!$ has been chosen (see §II B; but similar values for the viscosity result from $g(n_A) = \delta_{n_A,1}$ (see §II D), $g(n_A) = 1$, and the rigid state model $g(n_A) = \delta_{n_A, N_{\mathbf{a}}}$). This gives the known conditional transition probabilities for a rigid state transition, $n_A = N_{\mathbf{a}}$.

With this conditional transition probability, the average rate of change of momentum in the direction α for the subset $A \in \mathbf{a}$ to leading order is

$$\langle \dot{p}_A^0 \rangle = \frac{n_A \Delta_p}{\tau} \text{sign}(\tau F_{A,\alpha}) \lambda_{A,\alpha} \frac{n_A! (N_{\mathbf{a}} - n_A)!}{N_{\mathbf{a}}!}. \quad (2.14)$$

The classical regime is defined as $N_{\mathbf{a}} = n_A = 1$, and in order to satisfy Newton's second law of motion in this case we must have

$$\lambda_{A,\alpha} \equiv \frac{|\tau F_{A,\alpha}|}{\Delta_p}. \quad (2.15)$$

In the classical regime $\mathbf{F}_{\mathbf{a}} = \mathbf{F}_A = \mathbf{f}_j$ for $j \in A \in \mathbf{a}$.

With this result for $\lambda_{A,\alpha}$ and the conditional transition probability, Newton's second law is *not* satisfied in the quantum condensed regime. (As a consequence neither energy nor momentum are conserved, which is not unexpected as these results apply to an *open* quantum subsystem; see §II B.) Specifically, this says that for a highly occupied momentum state the rate of change of momentum for most subsets is much less than the classical prediction for a given applied force. The greatest reduction occurs when $n_A = N_{\mathbf{a}}/2$, in which case it is $\mathcal{O}(2^{-N_{\mathbf{a}}})$. Typically for low lying momentum states $N_{\mathbf{a}} = \mathcal{O}(10^2)$, and so this reduction is quite significant, exponentially small in fact. If the entire state attempts the transition as a rigid body with $n_A = N_{\mathbf{a}}$, then the combinatorial coefficient is unity and there is no reduction from the classical law. If an individual boson attempts the transition, $n_A = 1$, then its rate of change of momentum is reduced by a factor of $N_{\mathbf{a}}^{-1}$ from the value given by Newton's second law of motion.

In summary, for a given shared non-local force and a given subset, transitions from a momentum state are more frequent if the subset is the entire momentum state than if it consists of a fraction of the bosons in the state. But there are $(N_{\mathbf{a}} - 1)(N_{\mathbf{a}} - 1)!$ ways of choosing subsets that are not the entire state. Hence the vast majority of uniformly chosen subsets result in an exponentially reduced rate of change of momentum. But of course this all depends on the size distribution of the subsets, and this is derived in the following §IID.

Since superfluid flow consists selectively of bosons in highly occupied states, this says that the rate of change of their momentum is exponentially reduced. It follows that there is a direct connection between the conservation of entropy on an adiabatic trajectory, the reduction in the rate of change of momentum in the condensed regime, and the loss of shear viscosity in superfluidity.

A second contribution to the reduction in the rate of change of momentum of a subset is the shared non-local force of the subset, $n_A \mathbf{F}_A = \sum_{j \in A} \mathbf{f}_j$. This shared non-local force is a consequence of the permutations of the bosons in the momentum state. The magnitude of the change due to this for the momentum state scales with $n_A^{1/2}$, whereas the dissipative effects on the classical shear viscosity of individual momentum changes scale with n_A . This effect is largest for the largest subsets, but is non-existent for individual transitions (see next). This non-local sharing effect reduces the rate of change of momentum in shear flow from its classical value. The combinatorial effect of the occupation entropy and the effect of the non-local sharing of the forces explain at the molecular level the reduction in viscosity in the condensed superfluid.

D. Distribution of Subset Size

Let $\wp(n_A | N_{\mathbf{a}})$ be the probability of a subset of size n_A irrespective of its composition being involved in a transition from the momentum state containing $N_{\mathbf{a}}$ bosons. We now incorporate this into the unconditional transition probability. As in the preceding section, microscopic reversibility yields

$$\begin{aligned} & \wp(\mathbf{\Gamma}' | \mathbf{\Gamma}; n_A, \tau) \wp(\mathbf{\Gamma}) \wp(n_A | N_{\mathbf{a}}) \\ &= \wp(\mathbf{\Gamma}^\dagger | \mathbf{\Gamma}'^\dagger; n_A, \tau) \wp(\mathbf{\Gamma}'^\dagger) \wp(n_A | N'_{\mathbf{a}'_\alpha}). \end{aligned} \quad (2.16)$$

In the conjugate system, $N_{-\mathbf{a}} = N_{\mathbf{a}}$. We write $N'_{\mathbf{a}} = N_{\mathbf{a}} - n_A$ and $N'_{\mathbf{a}'_\alpha} = N_{\mathbf{a}'_\alpha} + n_A$.

The current conditional transition probability given in §IIC remains valid if the size probability cancels here,

$$\wp(n_A | N_{\mathbf{a}}) = \wp(n_A | N'_{\mathbf{a}'_\alpha}). \quad (2.17)$$

In general $N_{\mathbf{a}} \neq N'_{\mathbf{a}'_\alpha}$, and in view of the fact that the respective normalization constants in general depend upon each occupancy, and also the facts that $N_{\mathbf{a}} \geq 1$ and $N'_{\mathbf{a}'_\alpha} \geq 1$, the only way to ensure equality here is to choose

$$\wp(n_A | N_{\mathbf{a}}) = \delta_{n_A, 1}. \quad (2.18)$$

This is equivalent to choosing $g(n_A) = \delta_{n_A, 1}$ in Eq. (2.13), so that the conditional transition probability for boson $j \in \mathbf{a}$ becomes

$$\begin{aligned} & \wp_j(\mathbf{a}'_{j\alpha} | \mathbf{a}, N_{\mathbf{a}}) \\ &= \frac{|\tau f_{j\alpha}|}{N_{\mathbf{a}} \Delta_p} \left\{ 1 - \frac{\beta \Delta_p}{2m} \text{sign}(\tau f_{j\alpha}) a_\alpha + \frac{\beta \tau a_\alpha}{2m} f_{j\alpha} \right\}. \end{aligned} \quad (2.19)$$

Here $\mathbf{a}'_{j\alpha} = \mathbf{a} + \text{sign}(\tau f_{j\alpha}) \Delta_p \hat{\mathbf{x}}_\alpha$. Sequential transitions for each component and for each boson in the momentum state are attempted at each time step. There appears to be little difference in whether the occupancy is updated after each successful transition, or only at the end of the time step. There also appears little difference if the quadratic term in the change in kinetic energy is added. And it is also possible to use the exponential form of the term in braces.

The restriction to individual transitions, $g(n_A) = \delta_{n_A, 1}$, means that the damping of the rate of change of momentum is polynomial rather than exponential, $\propto N_{\mathbf{a}}^{-1}$. Since the occupancy of low-lying momentum states can be $\mathcal{O}(10^2)$ below the condensation transition, this is still a significant reduction, and it appears sufficient to be interpreted as the origin of superfluidity.

E. Dissipative Transition

The dissipative transitions act like a thermostat and provide another mechanism for the change in occupancy of the momentum states and for the equilibration of the occupancy distribution. For this I randomly or sequentially choose a boson from the N bosons in the subsystem, say j . I use the following conditional transition probability for the 27 near neighbor states \mathbf{a}' (including the original state \mathbf{a}). The block of N individual attempted transitions is performed typically once every 10 time steps, although less frequent attempts would probably suffice.

The dissipative transition is irreversible, which means that the forward and backward unconditional transitions are equally likely. Hence for the transition to a neighboring momentum state $\mathbf{a} \xrightarrow{j} \mathbf{a}'$, the ratio of conditional transition probabilities is

$$\begin{aligned} \frac{\wp_j(\mathbf{a}' | \mathbf{a})}{\wp_j(\mathbf{a} | \mathbf{a}')} &= \frac{\wp_j(\mathbf{a}')}{\wp_j(\mathbf{a})} \\ &= \frac{N_{\mathbf{a}'} + 1}{N_{\mathbf{a}}} \left[1 - \frac{\beta(a'^2 - a^2)}{2m} \right]. \end{aligned} \quad (2.20)$$

Here the change in kinetic energy has been expanded to quadratic order. This is satisfied by

$$\wp_j(\mathbf{a}' | \mathbf{a}) = \begin{cases} \frac{\varepsilon}{N_{\mathbf{a}}} \left[1 - \frac{\beta(a'^2 - a^2)}{4m} \right], & \mathbf{a}' \neq \mathbf{a} \\ 1 - \frac{26\varepsilon}{N_{\mathbf{a}}} + \frac{54\beta\Delta_p^2}{4m} \frac{\varepsilon}{N_{\mathbf{a}}}, & \mathbf{a}' = \mathbf{a}. \end{cases} \quad (2.21)$$

For the following results, $\varepsilon = 1/27$. The dissipative transitions were attempted one boson at a time, for all N

bosons in a cycle. A cycle of such attempts was made once every `skipcon` adiabatic time steps. These dissipative transitions roughly correspond to $r = 1$, $g(n_A) = \delta_{n_A,1}$, and $\lambda = 1/\text{skipcon}$.

The present algorithm has proven adequate to ensure the equilibrium distribution, although it is not actually clear that a dissipative thermostat is required because unlike the classical adiabatic equations of motion, temperature already appears in the present adiabatic conditional transition probability.

1. Ideal Boson Results

For ideal bosons, this second order dissipative transition algorithm for $T = 0.60$, $\rho = 0.8872$, and $N = 1,000$, gave for the occupancies of the first several low lying momentum states: $N_{000} = 85.9(43)$, (exact is 87.0), $N_{001} = 16.1(3)$, (exact is 14.5), $N_{011} = 8.2(1)$, (exact is 7.73), $N_{111} = 5.39(4)$, (exact is 5.17), $N_{002} = 3.94(3)$, (exact is 3.83).

For $T = 0.60$, $\rho = 0.8872$, and $N = 10,000$, the results were $N_{000} = 138.2(284)$, (exact is 138.0), $N_{001} = 52.0(31)$, (exact is 51.9), $N_{011} = 33.3(8)$, (exact is 31.8), $N_{111} = 23.5(5)$, (exact is 22.8), $N_{002} = 18.3(6)$, (exact is 17.8). These improve significantly the results of the linear algorithm given in earlier versions of this paper.

F. Viscosity Time Correlation Function

The shear viscosity can be expressed as an integral of the momentum-moment time-correlation function (Attard 2012a Eq. (9.117)),

$$\eta_{\alpha\gamma}(t) = \frac{1}{2Vk_B T} \int_{-t}^t dt' \left\langle \dot{P}_{\alpha\gamma}^0(\Gamma) \dot{P}_{\alpha\gamma}^0(\Gamma(t'|\Gamma, 0)) \right\rangle. \quad (2.22)$$

It was Onsager (1931) who originally gave the relationship between the transport coefficients and the time correlation functions. It is therefore somewhat puzzling that this is called a Green-Kubo expression (Green 1954, Kubo 1966). The first α -moment of the γ -component of momentum is

$$P_{\alpha\gamma} = \sum_{j=1}^N q_{j\alpha} p_{j\gamma}. \quad (2.23)$$

The classical adiabatic rate of change of momentum moment is

$$\dot{P}_{\alpha\gamma}^0 = \frac{1}{m} \sum_{j=1}^N p_{j\alpha} p_{j\gamma} + \sum_{j=1}^N q_{j\alpha} f_{j\gamma}. \quad (2.24)$$

The force \mathbf{f}_j gives the classical rate of change of momentum of boson j . This can be cast in symmetric form using the gradient of the pair potential, in which form the minimum image convention can be applied.

In the condensed regime, the average rate of change of momentum for boson j to leading order is

$$\langle \dot{\mathbf{p}}_j^0 \rangle = \frac{1}{N_{\mathbf{p}_j}} \mathbf{f}_j. \quad (2.25)$$

This uses $g(n_A) = \delta_{n_A,1}$, Eq. (2.19). With this the adiabatic rate of change of the first momentum moment is

$$\begin{aligned} \underline{\dot{P}}^0 &= \frac{1}{m} \sum_{j=1}^N \mathbf{p}_j \mathbf{p}_j + \sum_{j=1}^N \mathbf{q}_j \frac{1}{N_{\mathbf{p}_j}} \mathbf{f}_j \\ &= \frac{1}{m} \sum_{j=1}^N \mathbf{p}_j \mathbf{p}_j + \frac{1}{2} \sum_{j,k} \tilde{\mathbf{q}}_{jk} \mathbf{f}_{j,k}. \end{aligned} \quad (2.26)$$

Here $\mathbf{f}_{j,k}$ is the force on boson j due to boson k , so that the total force on boson j is $\mathbf{f}_j = \sum_k \mathbf{f}_{j,k}$, and

$$\tilde{\mathbf{q}}_{jk} \equiv \frac{1}{N_{\mathbf{p}_j}} \mathbf{q}_j - \frac{1}{N_{\mathbf{p}_k}} \mathbf{q}_k. \quad (2.27)$$

Generally simulations are conducted with periodic boundary conditions, which give a homogeneous system. In the uncondensed regime, $N_{\mathbf{a}} = 1$ and $\tilde{\mathbf{q}}_{jk} = \mathbf{q}_{jk}$. The minimum image separation is $\mathbf{q}_{jk} = \mathbf{q}_{jk} - L * \text{ANINT}(\mathbf{q}_{jk}/L)$, where ANINT gives the nearest integer. This guarantees that $|q_{jk,\alpha}| \leq L/2$ and it is known to work in the classical case (ie. it gives a viscosity that is independent of system size). In the condensed regime, $N_{\mathbf{p}_j} \geq 1$, and so the minimum image convention can still be applied to $\tilde{\mathbf{q}}_{jk}$ with the same guarantee.

In the simulations, the adiabatic rate of change of the first momentum moment was calculated once every 75 time steps. The time correlation function was constructed and integrated to give the viscosity time function. This was averaged over the six components (three in the classical case) and the maximum value taken to be ‘the’ shear viscosity.

III. RESULTS

In what follows what is defined as the classical fluid is treated with the same algorithm as the quantum fluid but as if the momentum states were solely occupied. Hence individual transitions were attempted without the factor of $N_{\mathbf{a}}^{-1}$ in the conditional probability or in the rate of change of the first momentum moment in the shear viscosity. However, the momenta were still quantized and the adiabatic transitions were still stochastic, just as in the quantum case.

The Lennard-Jones pair potential was used,

$$u(r) = 4\epsilon \left[\frac{\sigma^{12}}{r^{12}} - \frac{\sigma^6}{r^6} \right]. \quad (3.1)$$

This was set to zero for $r > 3.5\sigma$. The molecular diameter for helium is $\sigma_{\text{He}} = 0.2556 \text{ nm}$ and the well-depth

is $\varepsilon_{\text{He}}/k_B = 10.22 \text{ J}$ (van Sciver 2012). The mass is $m_{\text{He}} = 4.003 \times 1.66054 \times 10^{-27} \text{ kg}$.

The results below are presented in dimensionless form: the temperature is $T^* = k_B T / \varepsilon_{\text{He}}$, the number density is $\rho^* = \rho \sigma_{\text{He}}^3$, the time step is $\tau^* = \tau / t_{\text{He}}$, the unit of time is $t_{\text{He}} = \sqrt{m_{\text{He}} \sigma_{\text{He}}^2 / \varepsilon_{\text{He}}}$, and the shear viscosity is $\eta^* = \eta \sigma_{\text{He}}^3 / \varepsilon_{\text{He}} t_{\text{He}}$.

A canonical system, most commonly with $N = 1,000$ Lennard-Jones atoms, was simulated with the above quantum molecular dynamics algorithm. The time step was $\tau^* = 2 \times 10^{-5}$. A block of N dissipative transitions was attempted once every 10 time steps. For the classical liquid this combination consistently gave a kinetic energy 5-7% lower than the exact value. The present parameters were judged acceptable even though a smaller time step or a larger system would have given more accurate results albeit at the cost of longer simulation times. More frequent dissipative transitions would also likely improve the classical kinetic temperature but at the cost of greater interference in the adiabatic evolution of the momentum moment. Averages were collected once every 75 time steps. The number of time steps in a run was $10 \times 4,000 \times 75$. A run took 24-30 hours on a desktop personal computer. Typically 4-8 runs were made at each thermodynamic point, although twelve were made in the classical cases at the lowest temperatures. The quoted statistical error is the larger of the error estimated from the fluctuations in 10 blocks of each run (averaged across the runs), or the standard deviation across the runs. There was usually little difference in the two estimates (but see below). The shear viscosity time function was estimated for $t^* \leq 6$, which meant that the time correlation function was covered ten times, and that in a single run 10×6 values were averaged at each time point for the quantum case, and 10×3 values in the classical case. In the quantum case the viscosity time function had more or less reached its maximum by $t = 6$. In the classical case the viscosity time function was extrapolated beyond $t = 6$ to its maximum value using a quadratic best fit. The quantum viscosity time function was rather flat and no extrapolation was made. The components of the quantized momentum were restricted to $p_{j\alpha}^2 / 2mk_B T \lesssim 20$.

The liquid saturation curve obtained in previous work was followed (Attard 2023a): $\{T^*, \rho^*\} = \{1.00, 0.7009\}$, $\{0.90, 0.7503\}$, $\{0.80, 0.8023\}$, $\{0.75, 0.8288\}$, $\{0.70, 0.8470\}$, $\{0.65, 0.8678\}$ and $\{0.60, 0.8872\}$.

Figure 1 shows the ground state occupancy on the saturation curve for the Lennard-Jones liquid. It can be seen that the simulated occupancy in the quantum liquid is in good agreement with the analytic result calculated for non-interacting bosons. Comparable if not better agreement holds for the first several excited momentum states. The ideal boson result should apply to interacting bosons on the far side of the λ -transition (Attard 2025 §5.3). The slightly larger than ideal value for the quantum liquid ground momentum state occupancy

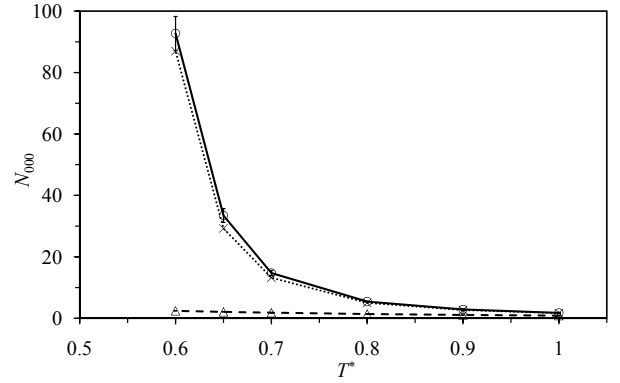


FIG. 1: Ground state occupancy in the saturated Lennard-Jones liquid. The circles are the quantum liquid, the triangles are the classical liquid, and the crosses are the exact result for ideal bosons. The error bars are less than the symbol size. The lines are an eye guide. Note that $T[K] = 10.22T^*$.

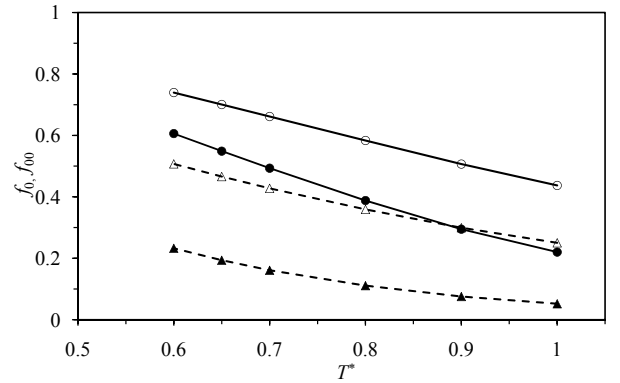


FIG. 2: Fraction of bosons condensed in the saturated Lennard-Jones liquid. The circles are the quantum liquid, the triangles are the classical liquid. The open symbols are f_0 , the fraction in states occupied by two or more bosons, and the filled symbols are f_{00} , the fraction in states occupied by three or more bosons. The error bars are less than the symbol size. The lines are an eye guide.

is probably a finite size effect.

At lower temperatures it can be seen that the occupancy in the quantum liquid is much larger than for the classical liquid. This is of course due to the role of the occupation entropy on the transition probability. However, the occupancy of the ground state in the quantum liquid is a small fraction of the total number of bosons in the subsystem. These fractions decrease with increasing subsystem size. Obviously this means that ground state condensation cannot account for the λ -transition or for superfluidity.

Figure 2 gives the fraction of condensed bosons in the subsystem. Condensed bosons were defined as those in multiply occupied states, with a threshold set at 2 for f_0 and 3 for f_{00} . In the quantum liquid at the lowest temperature studied about 74% of the bosons are in states with two or more, and about 61% are in states with three

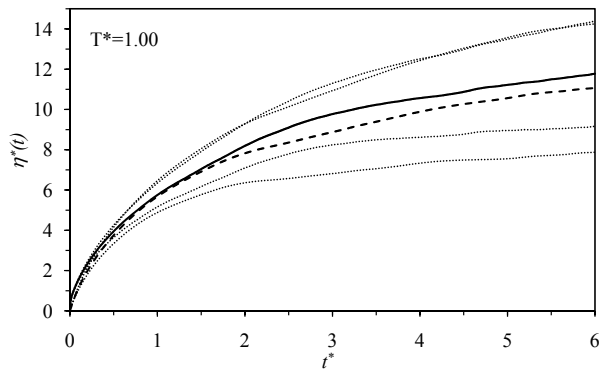


FIG. 3: Shear viscosity time function for the Lennard-Jones liquid at $T^* = 1.00$ and $\rho^* = 0.7009$. The solid curve is the quantum liquid, the dashed curve is the classical liquid, and the dotted curves give the 95% confidence level.

or more. In contrast the fraction for the classical liquid is 51% and 23%, respectively. These specific results are for $N = 1,000$, but other simulations show that these fractions are quite insensitive to the system size. The conclusion is that at these temperatures Bose-Einstein condensation is substantial, and that multiple momentum states are multiply occupied. That the majority of the bosons in the system can be considered to be condensed explains the macroscopic nature of the λ -transition and superfluidity.

It can be seen that at higher temperatures the condensation in the quantum liquid is approaching that in the classical liquid. However even at the highest temperature studied, $T^* = 1.00$, there is still excess condensation in the quantum liquid, $f_0^{\text{qu}} = 44\%$ compared to $f_0^{\text{cl}} = 25\%$. That there remains condensation in the quantum liquid well-above the superfluid transition temperature is likely due to the neglect in the present calculations of position permutation loops, which suppress condensation (Attard 2025 §3.2).

The kinetic energy per boson in the classical liquid is $\beta K/N = 1.4513(4)$ at $T^* = 1.00$ and $1.4048(2)$ at $T^* = 0.60$. The equipartition theorem gives the exact classical value as $3/2$. Clearly the present stochastic equations of motion that use the transition probability for quantized momentum are close to the continuum classical equations of motion. The discrepancy is probably an effect of finite size. The kinetic energy per boson in the quantum liquid is $\beta K/N = 1.2248(5)$ at $T^* = 1.00$ and $0.778(2)$ at $T^* = 0.60$. The decrease in kinetic energy with decreasing temperature is a manifestation of the increasing condensation in the quantum liquid that preferentially occurs in the low lying momentum states.

Figure 3 shows the shear viscosity time function for the quantum and classical liquids at the relatively high temperature of $T^* = 1.00$. The general features of the curves are that they rise from zero at $t^* = 0$ to reach a maximum or a plateau, in this case at about $t^* = 6$. This maximum value is taken to be ‘the’ shear viscosity.

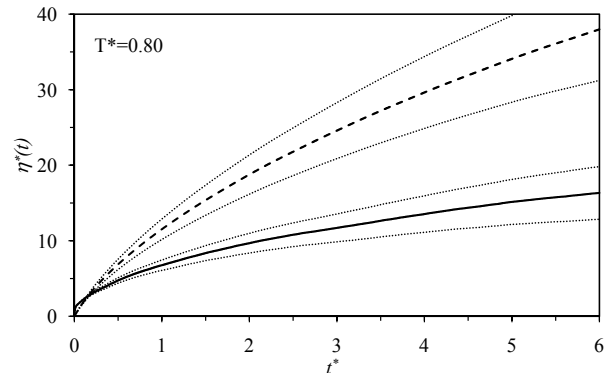


FIG. 4: As in the preceding figure but for $T^* = 0.80$ and $\rho^* = 0.8023$.

In this and lower temperatures the quantum viscosity is rather flat by $t^* = 6$; compare $\eta^{\text{qu}}(6) = 11.8(26)$ with the extrapolated maximum $\eta^{\text{qu}}(10.9) = 13.0$. At this highest temperature the same applies to the classical viscosity; compare $\eta^{\text{cl}}(6) = 11.1(32)$ with the extrapolated maximum $\eta^{\text{cl}}(7.3) = 11.3(34)$.

It can be seen that the viscosities of the quantum and classical liquids are statistically indistinguishable at this highest temperature studied. The fraction of condensed bosons in states with two or more bosons at this temperature is 44% for the quantum liquid and 25% for the classical liquid (Fig. 2). The average occupancy of momentum states containing two or more bosons in the quantum liquid was $\overline{N}_{\text{occ}}^{\text{qu},0} = 2.6258(5)$, and in the classical liquid it was $\overline{N}_{\text{occ}}^{\text{cl},0} = 2.1640(4)$. (The average occupancy of occupied states was $\overline{N}_{\text{occ}}^{\text{qu}} = 1.3712(3)$, and $\overline{N}_{\text{occ}}^{\text{cl}} = 1.1557(1)$, respectively.) Evidently at this temperature the occupation entropy has little effect on the occupation of momentum states. And the reduction in the rate of change of momentum due to occupancy has little effect on the viscosity.

The diffusion in the system was relatively small. The root mean square change in separation of a randomly chosen pair of bosons over the course of a run was $0.83(23)$ for the quantum liquid and $0.63(7)$ for the classical liquid. The statistical errors in the average potential energy and pressure were larger when estimated between runs rather than within a run. (Each run was started from an independently equilibrated configuration.) This suggests that the subsystem is somewhat glassy.

Figure 4 gives the shear viscosity time function at the lower temperature of $T^* = 0.80$. Note the change of scale. The viscosity of the quantum liquid is significantly lower than that of the classical liquid over virtually the whole domain. At very small times the quantum viscosity rises more quickly than the classical viscosity before flattening out. This effect was seen consistently in all the simulations, but the quantitative values in the small time regime appear sensitive to the frequency of the application of the dissipative thermostat. The extrapolated maximum vis-

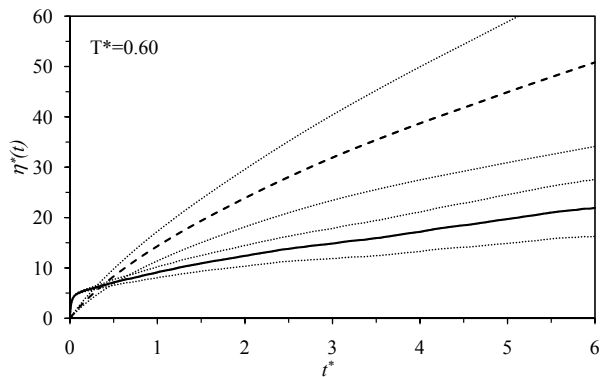


FIG. 5: As in the preceding figure but for $T^* = 0.60$ and $\rho^* = 0.8872$.

cosity of the classical liquid, $\eta^{\text{cl}}(12) = 49(13)$ (compare $\eta^{\text{cl}}(6) = 38.0(68)$), is much greater at this temperature than that at the higher temperature of the preceding figure. The root mean square change in separation was $0.45(8)$ for the quantum liquid and $0.59(9)$ for the classical liquid. The statistical errors in the average potential energy and pressure in the classical case were less when estimated from within a run as from between runs, suggesting a relatively glassy subsystem.

Figure 5 shows the viscosity for the lowest temperature studied, $T^* = 0.60$. Note the change of scale again. It can be seen that the classical viscosity is substantially larger than the quantum viscosity everywhere except at very short times. In the quantum case the viscosity time function is relatively flat at the terminus, which suggests that it is close to its maximum, $\eta^{\text{qu}}(6) = 21.9(57)$. In the classical case, there is enough curvature and slope to extrapolate to a maximum $\eta^{\text{cl}}(20) = 91(53)$, which is substantially larger than the value at the terminus, $\eta^{\text{cl}}(6) = 51(17)$.

The root mean square change in separation over a run was $0.31(6)$ for the quantum liquid and $0.25(5)$ for the classical liquid. The statistical errors in the average potential energy and pressure were smaller when estimated within a run than between runs. Again the conclusion is that the subsystem is somewhat glassy. If this is the case then it is remarkable that the shear viscosity has a finite value, and that it is so low for the quantum liquid.

Figure 6 shows the shear viscosity as a function of temperature for the saturated liquid. Based on the flatness of the curves, the quantum viscosity evaluated at $t = 6$ is close to its maximum value. The classical viscosity maximum is based on a quadratic best fit extrapolation. It can be seen that at higher temperatures the classical and quantum viscosities converge. At the lowest temperature studied the classical viscosity is about four times larger than the quantum viscosity. Whereas the classical viscosity increases by a factor of eight over the temperature range, the quantum viscosity only increases by a factor of two. The not quite doubling in condensation in the quantum liquid, Fig. 2, is sufficient to cancel almost

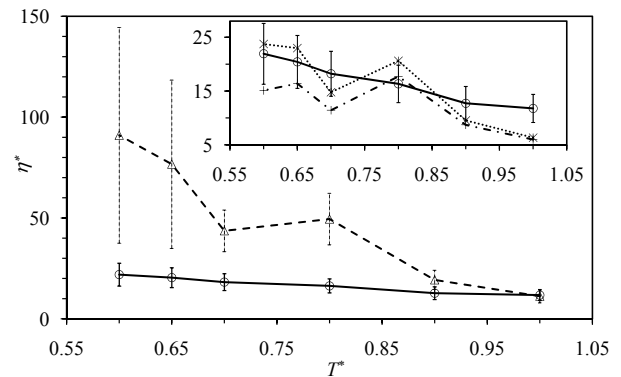


FIG. 6: Shear viscosity on the Lennard-Jones liquid saturation curve. The circles are for the quantum liquid $\eta^{\text{qu}}(6)$, the triangles are for the classical liquid $\eta_{\text{max}}^{\text{cl}}$. The error bars give the 95% confidence level, and the lines are an eye guide. **Inset.** Viscosity of the quantum liquid (circles) on a magnified scale compared to two predictions based on the classical viscosity. The asterisks connected by dotted lines are Eq. (3.2), and the plus symbols connected by dash-dot lines are Eq. (3.3). The statistical error of these is larger than that shown for the quantum liquid.

completely the classical viscosity increase. Evidently condensation reduces the rate of change of momentum via the factor of $1/N_{\text{a}}$, and this directly reduces the shear viscosity.

The inset to the figure includes results for

$$\eta_{\text{T}} = (1 - f_0^{\text{qu}})\eta_{\text{max}}^{\text{cl}}. \quad (3.2)$$

This viscosity is the analogue of the two-fluid model of superfluidity (Landau 1941, Tisza 1938), namely it is the fraction of uncondensed bosons (ie. those in singly-occupied momentum states) in the quantum liquid times the viscosity in the classical liquid (ie. the viscosity calculated as if all the bosons were in singly-occupied momentum states). Essentially it assumes that the viscosity of condensed bosons is zero, and it assumes that the actual viscosity is a linear combination of that of the individual components of a two-component mixture.

It can be seen that the two-fluid approximation is surprisingly good. For $T^* = 0.60$, $\rho^* = 0.8872$, the quantum viscosity is $\eta^{\text{qu}}(6) = 21.9(57)$, and the linear binary mixture result is $\eta_{\text{T}} = 24(14)$. For $T^* = 1.00$, $\rho^* = 0.7009$, the quantum viscosity is $\eta^{\text{qu}}(6) = 11.8(26)$, and the linear binary mixture result is $\eta_{\text{T}} = 6.3(19)$.

Of course in the present equations of motion the rate of change of momentum of condensed bosons is not zero, but is rather reduced by the occupancy of their respective momentum states. For the lowest temperature studied, $T^* = 0.60$, $\rho^* = 0.8872$, the average occupancy of momentum states in the quantum case was $\bar{N}_{\text{occ}} = 2.455(4)$. For such a small average occupancy it is perhaps surprising that the reduction of the rate of change of momentum is sufficient to reduce the superfluid viscosity by so much. In fact however a plausible model for the viscosity in the

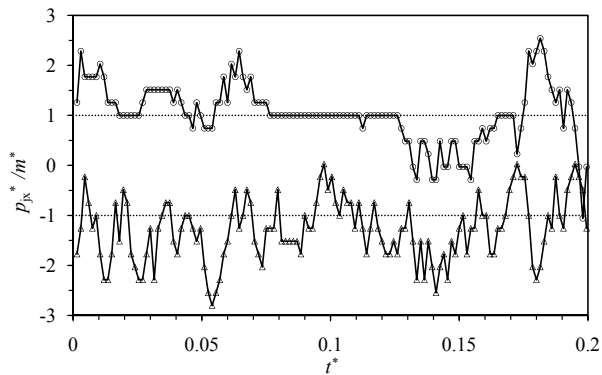


FIG. 7: Component of velocity of a typical boson on a trajectory at $T^* = 0.60$ and $\rho^* = 0.8872$, plotted once every 75 time steps. The circles are for the quantum liquid (offset by +1) and the triangles are for the classical liquid (offset by -1). The dotted lines give the zero momentum state for the component. The dimensionless spacing between momentum states is 0.26.

condensed regime is

$$\eta_A = \frac{1}{\overline{N}_{\text{occ}}^2} \eta_{\text{max}}^{\text{cl}}. \quad (3.3)$$

Here $\overline{N}_{\text{occ}} \equiv N/\overline{M}_{\text{occ}}$ is the average occupancy of occupied states, where $\overline{M}_{\text{occ}}$ is the number of occupied states. This factor gives the reduction in the rate of change of the first momentum moment in the force term. This neglects the diffusive (ie. ideal) contribution. This is squared because the viscosity time function is the *pair* time correlation of the rate of change of the first momentum moment. In the case $T^* = 0.60$ $\rho^* = 0.8872$ this formula gives $\eta_A = 15.1(89)$, to be compared with the two-fluid model $\eta_T = 23.7(139)$ and the actual simulated value $\eta^{\text{qu}}(6) = 21.9(57)$. At $T^* = 1.00$ $\rho^* = 0.7009$, with $\overline{N}_{\text{occ}} = 1.3712(3)$, the respective values are $\eta_A = 6.0(18)$, $\eta_T = 6.3(19)$, and $\eta^{\text{qu}}(6) = 11.8(26)$. It can be seen in the inset to Fig. 6 that the accuracy of this second model is comparable to that of the two-fluid model. This second model has a quantitative justification that does not insist that the viscosity of condensed bosons is zero. This formula explains how the seemingly small average occupancy of condensed bosons is sufficient to cause the reduction in superfluid viscosity comparable to the measured values.

Of course the virtue of molecular dynamics simulations such as the present is that they enable the classical and quantum viscosities, as well as the distribution of occupancies, to be computed at any thermodynamic state point, and in molecular detail. One wonders how useful the two-fluid model really is, since it does not appear possible to actually measure the individual viscosities or the individual mole fractions in a laboratory.

Figure 7 shows a quantum and classical trajectory for a component of momentum of a typical boson. It can be seen that there is a qualitative difference between the

trajectory in the quantum liquid and in the classical liquid. The quantum equations of motion yield a smoother curve, with smaller fluctuations, and noticeable stretches of constant momentum. These are correlated with the boson being in a highly occupied momentum state, which are noticeably the low-lying momentum states. On this portion of the quantum trajectory, the occupancy of the momentum state that this boson is in ranges up to 91, and averages 19.4. The conclusion is that the occupancy factor, $1/N_{\text{a}}$, damps the accelerations experienced by condensed bosons. It is not hard to imagine that the more frequent changes in momentum evident in the classical liquid dissipate momentum more efficiently and give rise to the usual viscosity of everyday experience.

IV. CONCLUSION

The two-fluid model of superfluidity (Landau 1941, Tisza 1938) holds that below the λ -transition helium is a mixture of helium I and helium II, with the former having normal viscosity and the latter being the superfluid with zero viscosity. For a bulk measurement, the shear viscosity is believed to be a linear combination of the two in proportion to their mole fraction. Helium II is believed to consist of bosons condensed into the ground energy state.

My definition of condensation is different namely that it occurs in the low-lying momentum states (Attard 2025). I also say that it is a simplification to divide the liquid into a mixture of two distinct fluids since there are multiple multiply-occupied states. Also, as few as two bosons in the same momentum state experience the effects permutation symmetry. Despite the simplicity of the two-fluid model, provided that condensation is interpreted as being into the low-lying momentum states, the results in Fig. 6 provide a measure of support for it.

Elsewhere (Attard 2025 §5.3) I have argued that on the far side of the λ -transition ^4He is dominated by momentum loops, which is to say permutations between bosons in the same momentum state. In this case the quantum statistical partition function factorizes into an ideal momentum part and a classical position configuration integral. This predicts that the occupancies of the momentum states are given by ideal statistics, for which the exact analytic results are known (Attard 2025 §2.2, Pathria 1972 §7.1). The present quantum stochastic molecular dynamics results for the occupancy agree with ideal statistics. This is a good test of the computational algorithm and programming.

The present analysis gives an explanation for the molecular origin of superfluidity. The shear viscosity is much reduced or practically zero for condensed bosons because Newton's second law of motion does not hold: the rate of change of momentum due to an applied force is significantly smaller in the condensed compared to the non-condensed regime. These quantum molecular dynamics equations are necessary for the equilibrium sys-

tem to evolve at constant entropy, as demanded by fundamental statistical considerations (Attard 2012a Ch. 7), and as confirmed by the thermodynamic analysis of fountain pressure measurements of superfluid helium (Attard 2025 §4.6). In addition, for the case of a subset of bosons changing momentum state, the applied force effective on each individual boson is the shared non-local force, which is reduced from the individual classical force by averaging over the subset to which the boson belongs.

Although this paper has focussed on the formulation of a computational algorithm for the viscosity of a quantum liquid, it should not be assumed that the molecular equations of motion that are given are merely a numerical technique. The equations of motion yield real trajectories for particles, and there is reason to suppose that the transition probability reflects the underlying reality of nature. This of course has implications for the physical interpretation of quantum mechanics and of the universe. To which end I suggest

speculate, calculate, and mensurate. (4.1)

References

- Attard P 2012a *Non-equilibrium thermodynamics and statistical mechanics: Foundations and applications* (Oxford: Oxford University Press)
- Attard P 2018 Quantum statistical mechanics in classical phase space. Expressions for the multi-particle density, the average energy, and the virial pressure arXiv:1811.00730
- Attard P 2021 *Quantum Statistical Mechanics in Classical Phase Space* (Bristol: IOP Publishing)
- Attard P 2023a *Entropy beyond the Second Law: Thermodynamics and statistical mechanics for equilibrium, non-equilibrium, classical, and quantum systems* (Bristol: IOP Publishing, 2nd edition)
- Attard P 2023b Quantum stochastic molecular dynamics simulations of the viscosity of superfluid helium arXiv:2306.07538
- Attard P 2023d Hamilton's equations of motion from Schrödinger's equation arXiv:2309.03349
- Attard P 2025 *Understanding Bose-Einstein Condensation, Superfluidity, and High Temperature Superconductivity* (London: CRC Press)
- Bohm D 1952 A suggested interpretation of the quantum theory in terms of 'hidden' variables. I and II. *Phys. Rev.* **85** 166
- de Broglie L 1928 La nouvelle dynamique des quanta, in *Solvay* p. 105
- Caldeira A O and Leggett A J 1983 Quantum tunnelling in a dissipative system *Ann. Phys.* **149** 374
- Goldstein S 2024 Bohmian mechanics *The Stanford Encyclopedia of Philosophy* (Summer 2024 Edition), E N Zalta and U Nodelman (eds.) URL = <https://plato.stanford.edu/archives/sum2024/entries/qm-bohm/>
- Green M S 1954 Markoff random processes and the statistical mechanics of time-dependent phenomena. II. Irreversible processes in fluids. *J. Chem. Phys.* **23**, 298
- Joos E and Zeh H D 1985 The emergence of classical properties through interaction with the environment *Z. Phys. B* **59** 223
- Kubo R 1966 The fluctuation-dissipation theorem *Rep. Prog. Phys.* **29** 255
- Landau L D 1941 Theory of the superfluidity of helium II *Phys. Rev.* **60** 356
- Mermin D 1989 What's wrong with this pillow *Physics Today* **42** 9
- Mermin D 2004 Could Feynman have said this *Physics Today* **57** 10
- Merzbacher E 1970 *Quantum Mechanics* 2nd edn (New York: Wiley)
- Messiah A 1961 *Quantum Mechanics* (Amsterdam: North-Holland volumes 1 and 2)
- Onsager L (1931) Reciprocal relations in irreversible processes. I. *Phys. Rev.* **37** 405. Reciprocal relations in irreversible processes. II. *Phys. Rev.* **38** 2265
- Pathria R K 1972 *Statistical Mechanics* (Oxford: Pergamon Press)
- Schlosshauer M 2005 Decoherence, the measurement problem, and interpretations of quantum mechanics arXiv:quant-ph/0312059v4
- van Sciver S W 2012 *Helium Cryogenics* (New York: Springer 2nd edition)
- Tisza L 1938 Transport phenomena in helium II *Nature* **141** 913
- Zurek W H 1991 Decoherence and the transition from quantum to classical *Phys. Today* **44** 36
- Zurek W H, Cucchietti F M, and Paz J P 2003 Gaussian decoherence from random spin environments arXiv:quant-ph/0312207.

Appendix A: Occupation of energy states?

The text invoked the occupation of low-lying momentum states. This contrasts with the conventional understanding of Bose-Einstein condensation, which maintains that condensation occurs into the ground energy state. This appendix proves that for interacting bosons the occupation of energy states is undefined.

Consider a system of N interacting bosons, which, for simplicity, has just two energy states with energy per boson e_1 and e_2 . If the occupancy picture is valid then the energy eigenvalues are of the form $E = N_1 e_1 + N_2 e_2$,

where N_a is the number of bosons in state a . The energies per boson, e_1 and e_2 , must be independent of occupancy.

If I add an extra boson and place it in the first state, $N \Rightarrow N + 1$, $N_1 \Rightarrow N_1 + 1$, then the second state must be unaffected. This implies that the eigenfunction of the second state must be independent of the new particle and its position. Hence the energy eigenfunction must factorize into those of the two states,

$$\phi_{N_1, N_2}(\mathbf{q}^{N_1}, \mathbf{q}^{N_2}) = \phi_{1; N_1}(\mathbf{q}^{N_1}) \phi_{2; N_2}(\mathbf{q}^{N_2}). \quad (\text{A.1})$$

This implies the energy eigenvalue equations

$$\begin{aligned} \hat{\mathcal{H}}_{1; N_1}(\mathbf{q}^{N_1}) \phi_{1; N_1}(\mathbf{q}^{N_1}) &= N_1 e_1 \phi_{1; N_1}(\mathbf{q}^{N_1}) \\ \hat{\mathcal{H}}_{2; N_2}(\mathbf{q}^{N_2}) \phi_{2; N_2}(\mathbf{q}^{N_2}) &= N_2 e_2 \phi_{2; N_2}(\mathbf{q}^{N_2}). \end{aligned} \quad (\text{A.2})$$

But these require the total Hamiltonian operator to be the sum of the individual Hamiltonian operators

$$\hat{\mathcal{H}}(\mathbf{q}^N) = \hat{\mathcal{H}}_{1; N_1}(\mathbf{q}^{N_1}) + \hat{\mathcal{H}}_{2; N_2}(\mathbf{q}^{N_2}). \quad (\text{A.3})$$

The interaction potential energy precludes this, $U(\mathbf{q}^N) \neq U(\mathbf{q}^{N_1}) + U(\mathbf{q}^{N_2})$.

There is an alternative way to see why factorization is forbidden by interaction. Using an abbreviated notation and assuming a factorized eigenfunction the energy eigenvalue equation is

$$\hat{\mathcal{H}}(\mathbf{q}_1, \mathbf{q}_2) \phi_1(\mathbf{q}_1) \phi_2(\mathbf{q}_2) = [E_1 + E_2] \phi_1(\mathbf{q}_1) \phi_2(\mathbf{q}_2), \quad (\text{A.4})$$

or

$$\frac{\hat{\mathcal{K}}(\mathbf{q}_1) \phi_1(\mathbf{q}_1)}{\phi_1(\mathbf{q}_1)} + \frac{\hat{\mathcal{K}}(\mathbf{q}_2) \phi_2(\mathbf{q}_2)}{\phi_2(\mathbf{q}_2)} + U(\mathbf{q}_1, \mathbf{q}_2) = E_1 + E_2. \quad (\text{A.5})$$

This follows since the kinetic energy operator is the sum of single-particle operators. Adding and subtracting this equation for states \mathbf{q}'_1 and \mathbf{q}'_2 gives

$$U(\mathbf{q}_1, \mathbf{q}_2) - U(\mathbf{q}'_1, \mathbf{q}_2) - U(\mathbf{q}_1, \mathbf{q}'_2) + U(\mathbf{q}'_1, \mathbf{q}'_2) = 0. \quad (\text{A.6})$$

But for nearby states this is just the second cross derivative of the potential, $(\mathbf{q}'_2 - \mathbf{q}_2)(\mathbf{q}'_1 - \mathbf{q}_1) : \nabla_1 \nabla_2 U(\mathbf{q}_1, \mathbf{q}_2)$. By definition this is non-zero for interacting particles. This proves that a factorized energy eigenfunction can only hold for non-interacting particles.

I conclude that it is meaningless to speak of the occupation of energy states for interacting particles.

Appendix B: Momentum eigenfunctions

In the text, and indeed in all of my work on quantum statistical mechanics from the beginning (Attard 2018, 2021), I take the momentum eigenfunctions to be (normalized, unsymmetrized)

$$\phi_{\mathbf{p}}(\mathbf{q}) = \frac{1}{V^{N/2}} e^{-\mathbf{q} \cdot \mathbf{p} / i\hbar}. \quad (\text{B.1})$$

The spacing between momentum states is $\Delta_p = 2\pi\hbar/L$, where L is the edge length of the cubic subsystem, the volume being $V = L^3$, and there are N bosons in the subsystem. Where does this come from?

It is clear that this is an eigenfunction of the momentum operator, $\hat{\mathbf{p}} = -i\hbar \nabla_{\mathbf{q}}$. It is also clear that this is periodic, $\phi_{\mathbf{p}}(\mathbf{q} + L\hat{\mathbf{x}}_{j\alpha}) = \phi_{\mathbf{p}}(\mathbf{q})$. But this on its own is a little strange because the physical system being dealt with does not consist of a set of periodic replicas of the subsystem. One would have guessed that the boundary condition should instead be that the wave function vanished on the boundary of the subsystem.

The reason for this form is that it ensures that the momentum operator is Hermitian, which is a fundamental requirement of quantum mechanics for an operator that represents a physical observable (Merzbacher 1970 Messiah 1961). To see this note that for periodic wave functions,

$$\begin{aligned} \int_V d\mathbf{q} \psi_1(\mathbf{q})^* \hat{\mathbf{p}} \psi_2(\mathbf{q}) &= -i\hbar \psi_1(\mathbf{q})^* \psi_2(\mathbf{q}) \Big|_{-L/2}^{L/2} \\ &\quad + i\hbar \int_V d\mathbf{q} (\nabla_{\mathbf{q}} \psi_1(\mathbf{q})^*) \psi_2(\mathbf{q}) \\ &= \int_V d\mathbf{q} (\hat{\mathbf{p}} \psi_1(\mathbf{q}))^* \psi_2(\mathbf{q}) \\ &\equiv \int_V d\mathbf{q} \psi_1(\mathbf{q})^* \hat{\mathbf{p}}^\dagger \psi_2(\mathbf{q}). \end{aligned} \quad (\text{B.2})$$

The integrated part vanishes on the boundary because of the periodicity, for example $\psi(-L/2, y_j, z_j) = \psi(L/2, y_j, z_j)$. The momentum eigenfunctions above form a complete basis set for such periodic wave functions. This links the quantization of the momentum states, which holds for a finite sized system, to the Hermitian nature of the momentum operator.